J. Membrane Biol. 141, 7–19 (1994)

The Journal of
Membrane
Biology

A Chloride Channel Reconstituted From Fetal Rat Brain Growth Cones

J.A. DeBin[1], M.R. Wood[2], K.H. Pfenninger[2], G.R. Strichartz[1]

[1]Anesthesia Research Laboratories of The Brigham and Women's Hospital and the Department of Biological Chemistry and Molecular Pharmacology, Harvard Medical School, Boston, Massachusetts 02115

[2]Department of Cellular and Structural Biology, University of Colorado School of Medicine, Health Sciences Center, Denver, Colorado 80262

Received: 11 November 1992/Revised: 9 March 1994

Abstract. Chloride channels were reconstituted into planar lipid bilayers isolated from a preparation of growth cone particles (GCPs) isolated from fetal rat brain. One type of channel was predominantly seen and some of its biophysical and pharmacological properties were studied. The single channel *i-V* relationship was curvilinear with a chord conductance of 75 pS at +30 mV in symmetric 200 mM NaCl solutions buffered with phosphate. The channel was inactivated by depolarization, and this inactivation was reversed rapidly upon returning to −25 mV. The Cl^- channel was significantly permeant to Na^+ ions ($P_{Na}/P_{Cl} = 0.26$), and the relative halide permeabilities were determined to be: I(1.92) > Br(1.73) > Cl(1.0) > F(0.34). The channel was inhibited by the common stilbene compounds (DIDS, SITS, DNDS), as well as by Zn^{2+} ions and an indanyloxyacetic acid derivative. A developmental role for the GCP Cl^- channel is suggested by the observation that adult rat brain synaptosomal membranes were nearly devoid of this type of Cl^- channel.

Key words: Anion channel — Chloride channel — Growth cone — DIDS — SITS — DNDS

Introduction

Although chloride channels have been described in most cell types, their physiological relevance is just beginning to be understood. Chloride channels may be broadly categorized into three major groups; ligand-gated, Ca^{2+}-gated, and ligand-independent. The GABA- and glycine-activated Cl^- channels of the vertebrate nervous system (Krnjevic, 1974) and arthropod muscle (Takeuchi & Takeuchi, 1964, 1966; Franke, Hatt & Dudel, 1986) are examples of ligand-activated Cl^- channels. A significant glutamate-activated Cl^- current is also found in arthropod muscle (Dudel et al., 1989; Sattele, 1992). Calcium-activated Cl^- currents have been described in neurons, epithelial cells, and pituitary cells (Owen, Segal & Barkers, 1984; Bader, Bertrand & Schlichter, 1987; Segal et al., 1987; Cliff & Frizell, 1990).

The third major class of Cl^- channels is that of the ligand-insensitive channels. These ion channels appear to be active spontaneously at most biologically relevant membrane potentials in the absence of any activating ligand (e.g., GABA, glycine) or ion (e.g., Ca^{2+}) and hence are sometimes referred to as "background" or "leak" channels. Leak channels are widely distributed, being found in neurons (Franciolini & Nonner, 1987; Yamamoto & Suzuki, 1987; Lukacs & Moczydlowski, 1990), skeletal muscle cells (Blatz & Magleby, 1983, 1985; Woll et al., 1987), and renal (Kolb et al., 1985), respiratory (Frizzell, 1988) and enteric epithelial cells (Bridges et al., 1987; Hayslett et al., 1987; Diener et al., 1989) of mammals, amphibians, molluscs, and insects. (Blatz & Magleby, 1983, 1985; Kolb, Brown & Murer, 1985; Woll et al., 1987; Frizzell, 1988; Gögelein, 1988; Diener et al., 1989).

The ligand-insensitive chloride channels found in mammalian skeletal muscle (Blatz & Magleby, 1985) are thought to be involved in maintaining resting membrane potential in the negative voltage range, and a similar function has been proposed for the Cl^- channels found in mammalian neurons (Franciolini & Nonner, 1987). In the epithelial cells lining the digestive and respiratory tracts, the transmembrane distribution of Cl^- is known to affect profoundly the quality of the glandular secretions (Frizzell, 1988). More recently, the

Correspondence to: G.R. Strichartz

Cl^- channels that control this distribution of Cl^- ions have been implicated as the site of the defect in the common inherited disease cystic fibrosis (Welsh et al., 1992).

While studying Na^+ channels reconstituted from sheared off fragments of embryonic rat brain growth cones (or growth cone particles, GCPs, Wood et al., 1992), we noted that a prominent feature of growth cone membranes is the abundance of Cl^- channels of the ligand-insensitive leak type described above. A developmental role for these channels was suggested by the observation that, in contrast to GCPs, synaptosomal preparations from mature brain were virtually devoid of these Cl^- channels. In response to this observation, a study of the biophysical and pharmacological properties of these channels was undertaken to understand their potential significance for development. In this paper we describe the gating properties, ion selectivity, and inhibition by stilbenes and other common blockers, of the Cl^- channels derived from GCPs following reconstitution into planar lipid bilayers. Some of these results have previously been reported in abstract form (DeBin & Strichartz, 1990).

Materials and Methods

Chloride Channel Reconstitution and Single Channel Recording

Chloride channels were reconstituted from fetal rat brain growth cones into planar lipid bilayers as described previously for Na^+ channels (Wood et al., 1992). The pertinent details of the reconstitution process are as follows: bilayers were formed across 0.25 mm diameter round apertures using phosphatidylcholine and phosphatidylethanolamine (2:1 ratio w/w, Avanti Polar Lipids, Alabaster, AL) at a total lipid concentration of 30 μg/μl decane. A volume of native membrane vesicles containing 10–25 μg of protein was pipetted near the aperture in the *cis* bath. Approximately 100 μl of solution was immediately removed from the *trans* bath to create a flow of solution, *cis* to *trans,* sweeping vesicles towards the aperture. A bilayer was then quickly formed to trap vesicles near the aperture. If no channel incorporation was seen within 10 min, stirring of the *cis* bath was initiated using a magnetic stir bar.

Cis and *trans* baths were connected through 1 M KCl-agar salt bridges and Ag/AgCl electrodes to a PC-501 patch clamp amplifier (Warner Inst., Hamden, CT). All experiments were performed in the voltage clamp mode. Data were initially stored on VCR tape using a Sony PCM-501 pulse code modulator. Select current traces were subsequently analyzed using the single channel programs provided by pCLAMP software (version 4.01 and 5.5, Axon Inst., Foster City, CA) using a PC's Limited AT/286 computer. All histograms shown are probability density histograms and were fit with least-squares functions using the Marquardt algorithm provided by pCLAMP.

All solutions during data acquisition (except for the determination of permeability ratios) were symmetrical NaCl 200 (in mM), 10 HEPES, 0.2 EGTA pH 7.4, or symmetric 200 NaCl, 10 phosphate, 0.2 citrate, pH 7.4 as indicated in the text and figure legends. A NaCl gradient, 200 mM *cis,* 50 mM *trans,* used to enhance fusion rates, was collapsed immediately after channel incorporation by adding concentrated NaCl to the *trans* bath.

Preparation of GCPs and Synaptosomes

Membrane preparations from fetal rat brains were isolated by a modification of the technique of Pfenninger et al. (1983; *cf.* Pfenninger et al., 1991). In brief, this procedure entails harvesting roughly six dozen fetal rat brains and homogenizing them in 0.32 M sucrose, 1 mM TES (*N*-tris(hydromethyl)methyl-2-aminoethane sulfonic acid), 1 mM $MgCl_2$, pH 7.3, with a tight-fitting Teflon pestle. The resulting *crude homogenate* is centrifuged at 1,660 × *g* for 15 min after which the supernatant (referred to as the low-speed supernatant or LSS) is recovered and loaded onto a discontinuous sucrose density gradient consisting of 0.83 M sucrose on a 2.66 M sucrose cushion. After centrifuging at 242,000 × g_{max} in a Beckman VTi50 rotor for 40 min, the GCPs at the 0.32/0.83 M interface (referred to as the A-Band) are collected, pelleted by centrifuging at 40,000 × g_{max} for 45 min and resuspended in 0.32 M sucrose for storage. B- and C-Band material is recovered from the 0.83/2.66 M sucrose interface.

In some cases, the final pelleting of the A-Band was onto a bed of Maxiden's Oil to produce a suspension of intact GCPs (*see* Table 1). All preparations (whether derived from fetal rat brains or adult rat brains—*see below*) were stored at −80°C for up to six months prior to use. The freezing-thawing process can be expected to cause some degree of rupture of the vesicular membranes.

Extensive electron microscopic examination has demonstrated that the A-Band material consists primarily of sheared off fragments of neuronal growth cones or growth cone particles (GCPs). The morphologic characteristics have been described in detail elsewhere (Pfenninger et al., 1983) and include the presence of mitochondria, smooth endoplasmic reticulum, and a variety of vesicular profiles. Stereologic point counting assays have determined the purity of this preparation to be upwards of 95% (Pfenninger et al., 1983).

Synaptosomes were prepared from the cortex of one or two adult rat brains using a discontinuous sucrose density gradient as described by Cohen et al. (1977).

Incorporation Rate Studies

The rate of incorporation of anion channels from various membrane preparations into the lipid bilayer was assayed under a standard set of conditions. All bilayers were of constant area (as assessed by capacitance measurements, 200–300 pF). The volume of vesicles (GCPs or synaptosomal) added to the *cis* bath contained 120 μg protein as determined by Lowry assay (Lowry et al., 1951). Bilayers were formed in the presence of a 200 mM *cis,* 50 mM *trans,* NaCl gradient, and were subjected to square wave pulses of 50 mV, alternating in polarity at 0.015 Hz. The *cis* bath was stirred at a constant rate with a small magnetic stir bar. If no channel activity was seen within 25 min, the membrane was ruptured, a new bilayer formed in its place, and the process continued.

Channels were identified as Cl^- selective based on the direction of current rectification at 0 mV applied potential in the presence of the 200 mM/50 mM NaCl gradient. All channels were briefly characterized by determining E_{rev}, measuring single channel currents at 0 mV, and by the observation of gating characteristics. Based on these criteria, only channels which exhibited the characteristics of the GCP anion channel were counted. This series of experiments was carried out over the course of several weeks, with each fraction being examined on at least three different days.

Open Channel Probability *vs.* Membrane Potential

For individual Cl^- channels, open channel probability was expressed as $P_o = t_o/(t_o + t_c)$. Mean open time (t_o) and mean closed time (t_c)

were determined from the average dwell time for the population of events, using pCLAMP software with 0.5 open current amplitude as the closed/opened criterion. To eliminate the consideration of rapid channel gating, a cut-off time of 100 msec was used for the detection of closures. Only the first five minutes of a gating record after a change in V_m were analyzed and used to determine the P_o *vs.* V_m relationship shown in Fig. 4.

Determination of Permeability Ratios

Values for P_{Na}/P_{Cl} were determined from E_{rev} measurements in the presence of a 200 mM/50 mM NaCl gradient using Eq. (A1) of the Appendix. Activity coefficients (*not shown in* Eqs. A1 or A2) were obtained from Robinson and Stokes (1959). The permeability ratio of test anion to Cl^- (P_A/P_{Cl}) was determined by collapsing the 200/50 NaCl gradient by adding a small volume of the concentrated Na^+ salt of the test ion to increase the concentration of anions in the *trans* bath (which was either the intracellular or the extracellular bath) by 150 mM to a final concentration of 200 mM (Cl^- ion plus test anion). Reversal potentials were then measured in the presence of the test ion and P_A/P_{Cl} was determined by substituting the value previously determined for P_{Na}/P_{Cl} into Eq. (A1) and solving for P_A/P_{Cl}. The only exception to this was with phosphate, in which case the NaCl gradient was partially collapsed by adding Na^+ phosphate to 75 mM. Permeability ratios were calculated first for $HPO_4^=$ assuming that $H_2PO_4^-$ is impermeant, and then the converse was done for $H_2PO_4^-$. Because of the equilibrium between $H_2PO_4^-$ and $HPO_4^=$ at pH 7.4, a concentration of 29 mM was used for $H_2PO_4^-$, and 46 mM for $HPO_4^=$ in Eqs. (A1) and (A2). Permeability ratios for divalent anions were calculated using Eq. (A2) of the Appendix.

Chloride Channel Blockers

All drugs were added from concentrated stock solutions. DIDS (4,4′-diisothiocyanostilbene-2,2′-disulfonic acid) was purchased from Research Organics, Cleveland, OH, and DNDS (4,4′-dinitrostilbene-2,2′-disulfonic acid) from Pfaltz and Bauer, Waterbury, CT. Aqueous stocks of DIDS and DNDS were prepared fresh each day for use. The indanyloxyacetic acid derivative, 94-IAA, was added from ethanol stocks and was a generous gift of Dr. Donald Landry, Dept. of Medicine, Columbia University College of Physicians and Surgeons, NY. As a control, a volume of ethanol equal to that which was used to deliver 94-IAA was tested and found to be without effect on GCP anion channels.

For DNDS and 94-IAA, K_ds were defined by first determining i_c (single channel current amplitude in the absence of drug, i.e., control experiment), and i_d (current amplitude in the presence of drugs). Hill plots were constructed by defining the relative single channel current amplitude, i_r, as i_d/i_c and setting fractional occupancy (Y) equal to $1 - i_r$. Once a single binding site was established (from the Hill coefficients near unity), K_d was defined from occupancy *vs.* concentration curves as in Fig. 7. Concentration *vs.* occupancy curves were fit with hyperbolic functions using Sigmaplot software (version 3.1, Jandel Scientific, Sausalito, CA).

Results

Incorporation Rate Studies

Studies were designed to test the assumption that the origin of the GCP Cl^- channel is, in fact, the GCPs and not a contaminating membrane. If the GCP channel derives from the GCPs, then with each step of the purification process the Cl^- channel activity, as assessed by the rate of bilayer incorporation, should increase.

Chloride channels were identified as described in Materials and Methods. Only one type of Cl^- channel was routinely reconstituted from the GCPs. Large conductance Cl^- channels were only rarely (roughly one in every 50–100 incorporations) reconstituted from either GCPs or synaptosomes and were not studied in detail. The results of the incorporation rate studies are summarized in Table 1.

From the homogenate to the low-speed supernatant only a modest enhancement of Cl^- channel activity was seen. However, from the crude homogenate to the A-Band (i.e., GCPs suspended in the high-speed supernatant of the homogenate), an increase of nearly 10-fold is seen. Synaptosomes had virtually no Cl^- channels; in 890 min of observation only one small conductance Cl^- channel of the type described from GCPs was seen. The synaptosomes used for these experiments were pelleted in plain tubes unlike the crude homogenate, LSS and A-Band (GCP) material which were pelleted onto Maxiden's Oil. Therefore, to allow a comparison of synaptosome Cl^- channel activity with GCP Cl^- channel activity, the incorporation rate of Cl^- channels from GCPs pelleted in plain tubes is included in Table 1. These data indicate that Cl^- channel activity is 275 times greater in the GCPs than in the synaptosomes.

Chloride Channel Gating Characteristics

Figure 1 shows current records from the same GCP Cl^- channel at four different membrane potentials. Current-voltage curves were constructed for GCP Cl^- channels in symmetric 200 mM NaCl HEPES/EGTA. The results are shown in Fig. 2*A*. The *i-V* relationship is curvilinear, indicative of current rectification. GCP Cl^- channels were reconstituted in the bilayers in either of two possible orientations, i.e., current rectification from *cis* to *trans* bath or *trans* or *cis*. For the sake of simplicity of discussion, the channels were arbitrarily considered to be outwardly rectifying based on the observation that most rectifying Cl^- channels in identified membranes are outwardly rectifying (Gögelein, 1988; *see also* Discussion). Thus, with this assumption, chord conductances of 26.7 ± 1.7 pS (n = 3) at −30 mV and 36.0 ± 7.3 pS (n = 4) at +30 mV were recorded (both values ± SD). In Fig. 1 the current rectification is evident from a comparison of the current amplitudes at −20 and +20 mV and especially at −40 and +40 mV. Throughout this paper, the assumption concerning the rectification properties of the Cl^- channel will be used to define the intra- and extracellular channel surfaces. It should be emphasized that the true direction of current rectifi-

Table 1. Incorporation rate studies

Preparation	Incorp. rate[a] (hr^{-1})	Total observation time (min)
Crude homogenate	0.78 ± 0.30	758
LSS	1.04 ± 0.45	736
A-Band	6.29 ± 2.56	393
B-Band	1.16 ± 0.53	469
Pelleted synaptosomes	0.05 ± 0.11	890
Pelleted GCPs	13.79 ± 7.71	121

This is a summary of the rates of anion channel incorporation into planar bilayers from membranes at various stages during the preparation of GCPs from fetal brain. *See* Materials and Methods for a description of each fraction listed under "preparation." Crude homogenate, LSS (low speed supernatant) and A-Band are the parent fractions of GCPs. The A-Band material represents intact GCPs suspended in homogenate pelleted to remove soluble protein and resuspended. The B-Band contains the (non-GCP) balance of LSS particulates. Synaptosomes prepared from adult brain are shown for comparison. In the rightmost column is the total length of time spent waiting for channel incorporations from each preparation. [a] Means ± SEM. Protein (120 μg) in 4.0 ml of *cis* bath *under all* ***conditions*** of all membranes.

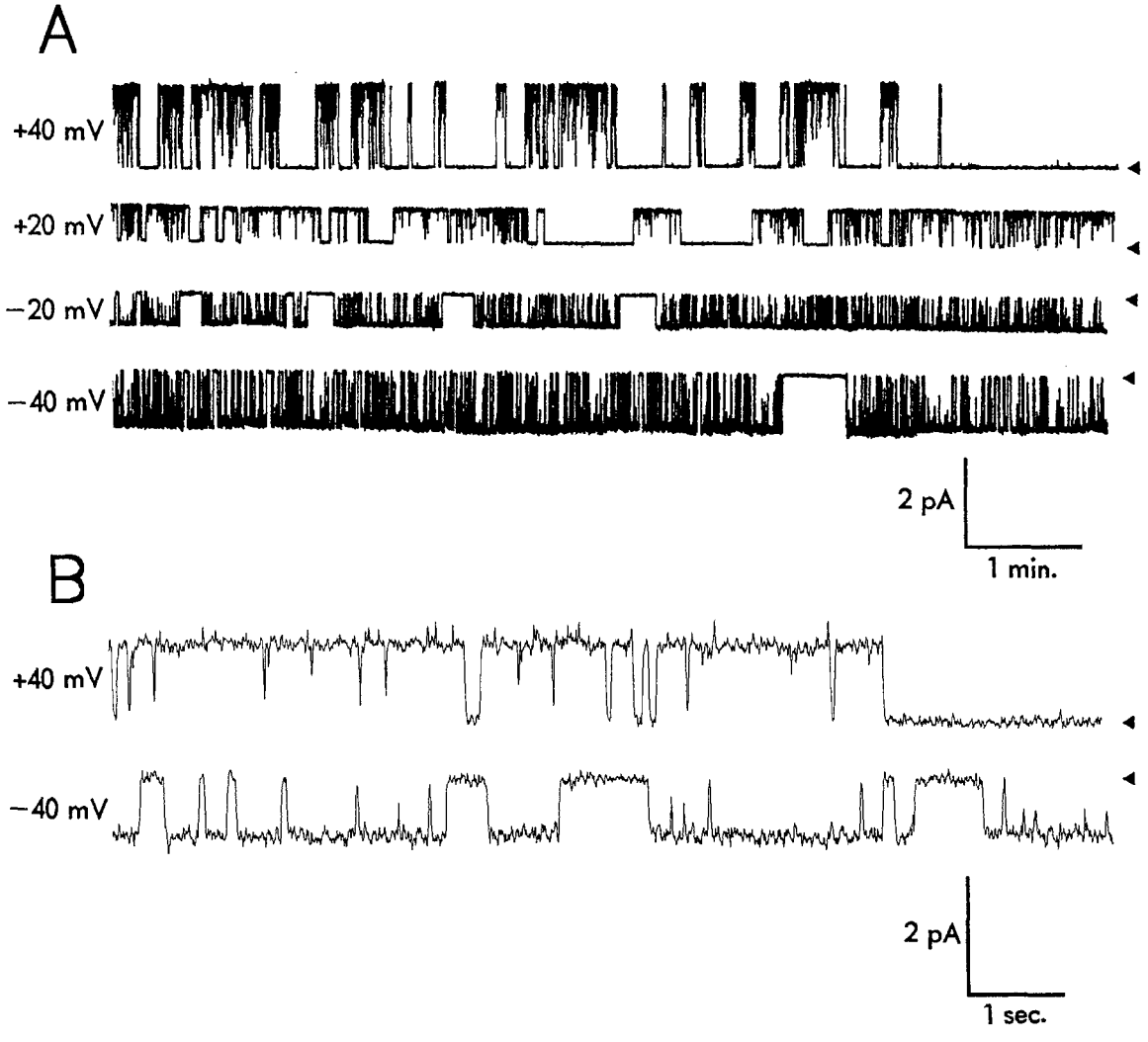

Fig. 1. Current fluctuations from GCP chloride channels. These current traces are from the same GCP anion channel held at either ±40 or ±20 mV, as indicated, in 200 mM NaCl, 10 mM HEPES, 0.2 mM EGTA. (*A*) Low time resolution current traces from strip chart records. (*B*) High time resolution traces plotted from digital recordings using pCLAMP. In all cases the closed, zero current level is indicated by the arrowhead at the right. Records at positive potentials run left to right, and at negative potentials right to left.

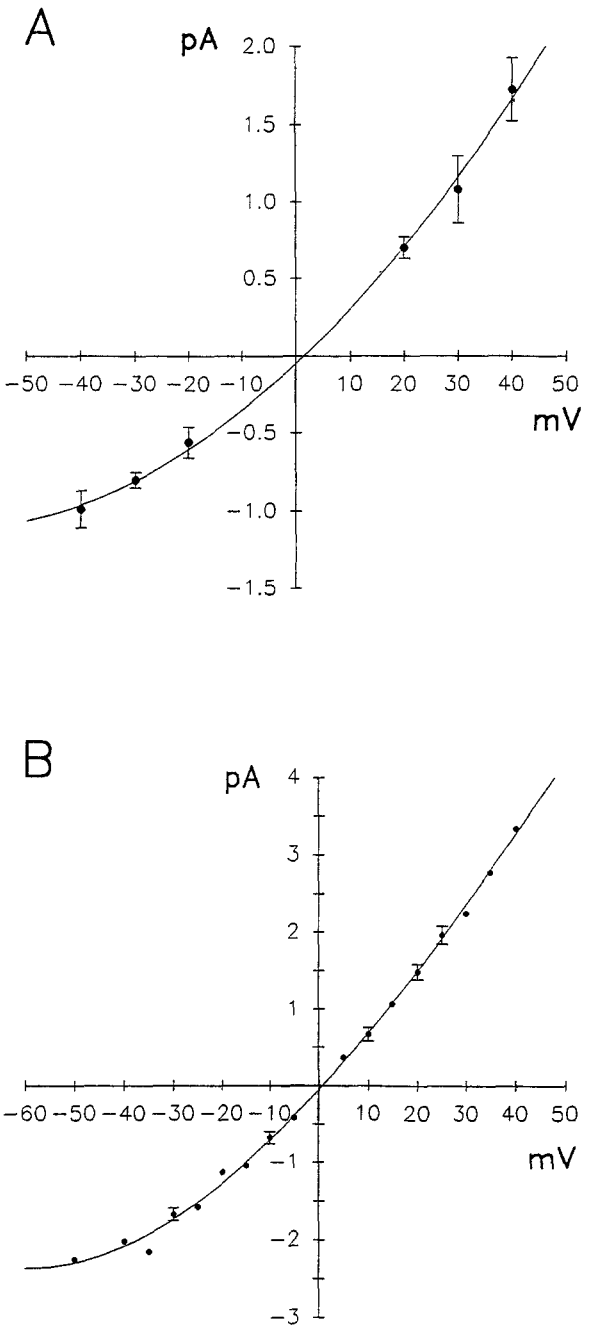

Fig. 2. Current-voltage relationships for GCP chloride channels. (*A*) The ionic conditions for the generation of this *i-V* curve were symmetrical: 200 mM NaCl, 10 mM HEPES, 0.2 mM EGTA. Each data point represents 3–8 determinations, and the scale bars represent standard deviations. The smooth curves drawn through the data points were third order polynomials fit to the data by regression analyses performed by Sigmaplot software. (*B*) Ionic conditions were symmetrical: 200 mM NaCl, 10 mM phosphate, 0.2 mM citrate, pH 7.4. Those points with error bars represent the means of 3–5 determinations, and those without error bars are the means of two determinations.

cation cannot be determined using channel reconstitution in bilayers.

When *i-V* curves were constructed in the presence of 200 mM NaCl, phosphate/citrate buffer, the current rectification was equally pronounced but the current magnitude was doubled at each voltage relative to that measured in the zwitterionic buffer (Fig. 2*B*). This indicates that Cl^- channels may be blocked by HEPES/EGTA buffer, as will be discussed below. The chord conductances in the presence of phosphate/citrate were 55.7 ± 2.7 pS (n = 3 ± SD) at −30 mV and 74.7 pS (n = 2) at +30 mV.

At all voltages, the Cl^- channels continuously fluctuate between the two well-defined open and closed states (Fig. 1). Subconductance states are not seen in the channel depicted in Fig. 1, and were *rarely* observed in any channels which were studied. Occasionally, some channels (roughly 1 in every 40 studied) did exhibit sudden changes in current amplitude to a level one-half the normal level. Such transitions to subconductance states were spontaneous, transient (lasting <60 sec), and could not be elicited by any experimental manipulations (e.g., changes in V_m) and therefore were not studied.

A comparison of the records in Fig. 1 reveals the greater frequency of short closings (<100 msec) at negative membrane potentials. Compared with channels held at positive potentials, the greater frequency of brief spontaneous closures at negative potentials could, in principle, explain the observed current rectification. If these closures are beyond the limits of detection at 50 Hz low pass (*see* figure legend), a reduction in mean current level may instead be observed. This possibility was examined by increasing the corner frequency of the filter to 200 Hz while examining several records. Up to 200 Hz, there was no increase in single channel current amplitude at any potential studied (+30 to −30 mV). Thus, it appears that the observed current rectification is an intrinsic property of the open, ion-conducting channel.

Closed time probability density histograms were generated for several channels at various voltages. Examples of these are shown in Fig. 3. The closed duration distributions were dominated by rapid closures at both +20 mV (Fig. 3*A*) and −40 mV (Fig. 3*B*). Closed time histograms were well fit by double exponential functions, but in all cases (the two shown in Figs. 3*A* and *B*, plus four other histograms from different channels) the faster of the two time constants was ≤10 msec. Considering that all records were filtered at 50 Hz low pass, the significance of this time constant is questionable. Given the constraints imposed by the bilayer instrumentation, a more extensive kinetic analysis was not attempted.

At positive membrane potentials, the frequency of long (>10 sec) closures increased dramatically. This is most clearly seen at +40 mV in Fig. 1. The inactivation of a GCP Cl^- channel can be seen at the end of the low time resolution current trace at +40 mV (Fig. 1*A*, top right). This inactivation with strong depolarization was a feature consistently observed in Cl^- channels

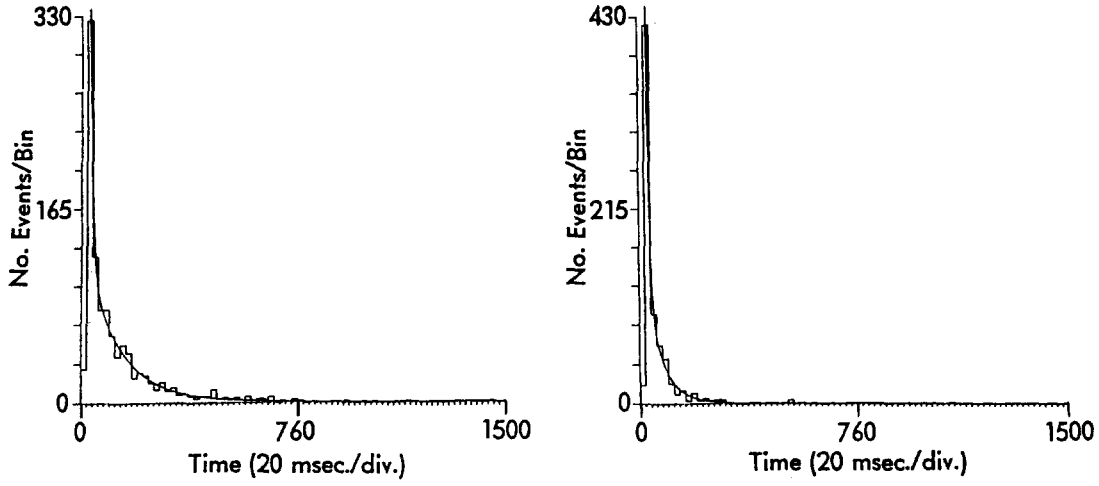

Fig. 3. Closed time histograms. (*A*) Probability density histograms were generated by pCLAMP software from data acquired from a GCP anion channel held at +20 mV. The ionic conditions were 200 mM NaCl, 10 mM HEPES, 0.2 mM EGTA. Records were filtered at 50 Hz, therefore the closed time histogram was fit from 20 msec on, with a double exponential function yielding time constants of 120.7 and 10.0 msec. There are a total of 1,079 events. (*B*) This histogram was generated from the same channel held at −40 mV, therefore all conditions are the same as stated for *A*. There are a total of 801 events, and the time constants for the fit of the closed time histogram were 51.9 and 7.2 msec.

isolated from the GCPs. The effects of this inactivation are evident in Fig. 4 which plots P_o *vs.* V_m. From −70 through +30 mV, P_o remains high, between 0.80 and 0.60, but declines abruptly between +30 and +40 mV, from *ca.* 0.75 to below 0.50. By the time +60 mV is reached, P_o has dropped to near zero.

The kinetics of depolarization-induced inactivation of a GCP Cl^- channel is demonstrated in Fig. 5. The current record runs from left to right. The channel initially resides primarily in the open state at −25 mV. Upon changing the membrane potential to +60 mV, the channel remains open for nearly 10 sec before entering into a prolonged closed period lasting >2 min. Upon return of the membrane potential to −25 mV, the inactivation is rapidly reversed. Although the time course at the millisecond scale is obscured by the larger bilayer capacitance transient, at the best determination the reversal of inactivation occurs within seconds. Some Cl^- channels required pulses to potentials more negative than −25 mV to reverse inactivation and all channels could be re-activated by pulsing to −100 to −125 mV for 5–10 sec.

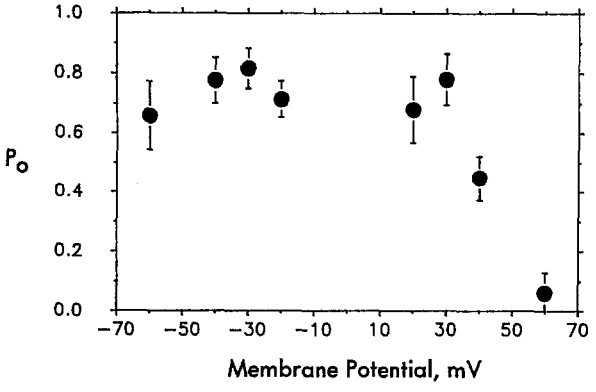

Fig. 4. Open channel probability as a function of membrane potential. The determination of P_o is described in Materials and Methods. Each data point represents the mean of 3–5 determinations from different GCP chloride channels. Error bars represent standard deviations.

Ion Permeation

The GCP Cl^- channels were permeant to all halide ions, multivalent anions, and at least one organic anion. The permeability-selectivity ratios, summarized in Table 2, were determined as described in Materials and Methods. The most striking result from these determinations is the remarkably high P_{Na}/P_{Cl} ratio which indicates that the channel does not discriminate well between such widely divergent atomic species as anions and Na^+ ions. However, because the P_{Na}/P_{Cl} ratios were determined under conditions in which a significant osmotic gradient was present across the bilayer (200 mM NaCl/50 mM NaCl, *see* Materials and Methods), the possibility existed that the unusually high P_{Na}/P_{Cl} could be due to a streaming potential as has been previously proposed (Franciolini & Nonner, 1987). To test this hypothesis, Cl^- channels were reconstituted and E_{rev} measurements were made from *i-V* curves in symmetrical 200 mM NaCl. By adding concentrated urea to one side of the bilayer, osmotic gradients equivalent to 500 mOsm were generated. Reversal potentials were then measured in the presence of urea and in two experiments

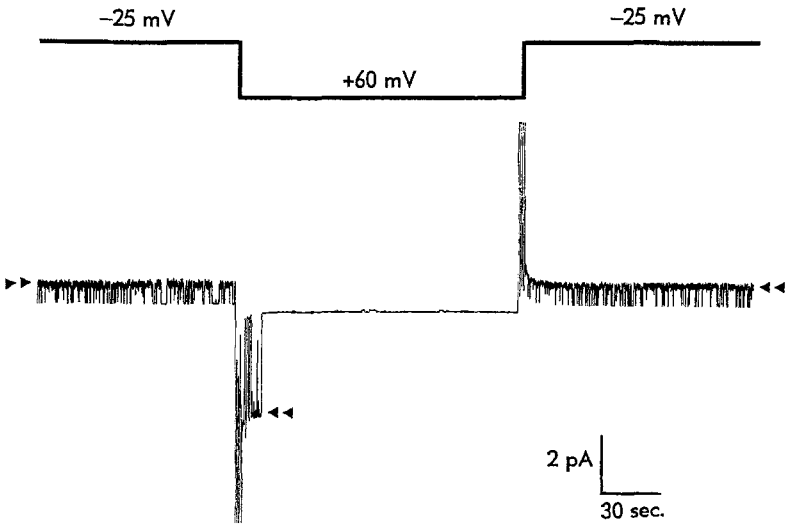

Fig. 5. GCP chloride channel inactivated by depolarization. This is a continuous current record from a GCP anion channel in symmetrical 200 mM NaCl, 10 mM HEPES, and 0.2 mM EGTA. The current record, taken from a strip chart recording, runs from left to right, and the open state is indicated by the double arrowhead at each voltage. Because this is a bilayer trace, a closing transition is upward at positive potentials, and downward at negative potentials. Applied membrane potential is indicated by the thick square wave above the current trace. Note the rapid reversal of inactivation upon changing from +60 to −25 mV.

Table 2. Permeability ratios for various anions and sodium

Test ion (A)	$P_A:P_{Cl}$	n
Na^+	0.26 ± 0.05	9
I^-	1.92 ± 0.07	3
Br^-	1.73 ± 0.49	4
Cl^-	1	
F^-	0.34	2
$H_2PO_4^-$	0.62 ± 0.20	3
$HPO_4^=$	0.16 ± 0.04	3
$Gluconate^-$	0.24	2
$SO_4^=$	0.57 ± 0.024	3
Na^+	0.21 ± 0.02[a]	4
I^-	2.27[a]	2
Br^-	1.95[a]	2

The ratios (±SD) for phosphate were calculated assuming that *either* the divalent *or* the monovalent forms are alone permeant in each case. ([a]) Ratios calculated from experiments performed in phosphate/citrate buffer; the other values are from HEPES/EGTA buffered solutions. The activity coefficient for caporate was used in determining the permeability ratio for gluconate.

found to be 1.7 and 4.4 mV. According to the Goldman, Hodgkin, Katz equation (Appendix), the E_{rev} for a perfectly selective Cl^- channel in 200/50 mM NaCl should be 35 mV. However, in nine experiments with a NaCl gradient in place, the mean E_{rev} potential was 18.33 ± 2.10 mV ($n = 9 \pm$ SD). Thus, streaming potential can at best account for only a small fraction of the observed deviations from perfect Cl^- selectivity.

Two values are given in Table 2 for P_{phos}/P_{Cl}. Because phosphate ion exists as an equilibrium between $H_2PO_4^-$ and $HPO_4^=$ at pH 7.4, either or both ionic species could be permeant. The ratios given in Table 2 are for the limiting conditions in which only one or the other ion is assumed to be permeant.

It was noted above in Chloride Channel Gating Characteristics that the *i-V* relationship differs in the presence of HEPES/EGTA as compared to phosphate/citrate. Current amplitudes in the presence of HEPES were half those in the presence of phosphate, indicating that the HEPES/EGTA buffer in some way inhibits the GCP Cl^- channel. Indeed, reports indicate that sulfate-containing buffering agents (e.g., HEPES and MOPS) inhibit a wide variety of Cl^- channels (Yamamoto & Suzuki, 1987; Hanrahan & Tabcharani, 1990).

To test for inhibition by HEPES, GCP Cl^- channels were reconstituted in the presence of phosphate/citrate buffer and subsequently exposed to the concentration of HEPES used during previous experiments (i.e., 10 mM). After the addition of 10 mM HEPES to each side of a bilayer, single channel current amplitudes were reduced to 60% of control at all voltages tested. The frequency of brief closings (<0.1 sec) did not appear to increase in the presence of HEPES and when the corner frequency of the filter was increased to over 200 Hz, no increase in single channel current amplitude was seen after the addition of HEPES. These results indicate that the time constant for block of the GCP Cl^- channel by HEPES is less than 5 msec. Thus, as previously reported (Yamamoto & Suzuki, 1987; Hanrahan & Tabcharani, 1990), HEPES induces a short-lived block of the open anion channel.

EGTA had little or no effect on single channel currents when present at the concentrations used for the experiments described in this paper (i.e., 200 μM). However, at higher concentrations (1 mM both sides of the bilayer), a modest reduction (*ca.* 20%) in current amplitude was seen.

The permeant phosphate anion (Table 2) caused no reduction in current amplitude when raised from 3 to 35 mM in two experiments. Likewise, citrate was without effect on current amplitude when present at up to 7 mM on both sides of the bilayer. Thus, phosphate/citrate was chosen as the buffering system for

some experiments to eliminate the blocking effects of HEPES.

In light of the effects of HEPES/EGTA on ion permeation through the GCP Cl^- channel, it was decided to repeat the determination of certain permeability ratios in the presence of phosphate/citrate buffer. At the bottom of Table 2, it can be seen that the P_{Na}/P_{Cl} was not substantially different when measured in phosphate/citrate buffer *vs.* HEPES/EGTA. Furthermore, the partial sequence $I^- > Br^- > Cl^-$ confirms that the GCP Cl^- channel still follows sequence I of Wright and Diamond (1977) when using phosphate/citrate as the buffer instead of HEPES/EGTA.

Inhibitors of the GCP Chloride Channel

The inhibition of GCP Cl^- channels by extracellularly applied DIDS is shown in Fig. 6. The block by DIDS results from two distinct effects; a progressive diminution in single channel current with an associated increase in flicker, and an increase in the frequency of long closures. Although it is unclear whether these effects are mechanistically related, they have previously been reported for the stilbene-induced block of Cl^- channels from brain (Nomura & Sokabe, 1991), lobster nerve (Lukacs & Moczydlowski, 1990), and fibroblasts (Bear, 1988). A similar inhibition of the GCP channel was seen in response to the application of 50 μM SITS.

DNDS induced a rapid, reversible channel block when applied to the extracellular surface of the GCP Cl^- channel (Fig. 7*A*). Hill plots were constructed (*not shown*) which yielded Hill coefficients of 0.88 and 0.92 at +25 and −25 mV, respectively (data from five experiments). Given one site for DNDS binding, K_ds of 1.80 and 4.22 μM (at +25 and −25 mV, respectively) were determined from occupancy *vs.* concentration curves. Each of the stilbene inhibitors (DIDS, SITS, and DNDS) gave approximately equal inhibition regardless of the side of the GCP Cl^- channel to which they were applied. The implication is that either there are sites of similar affinity on each side of the channel or that one common site can be reached by drug molecules permeating from either surface of the membrane.

When the membrane permeant inhibitor 94-IAA (Landry et al., 1989) was applied to *both* sides of the GCP Cl^- channel simultaneously, a rapid channel block was induced (Fig. 7*B*). Hill plots were generated as shown in Fig. 7*B* (center panel at bottom; data from two experiments) from which a Hill coefficient of 1.24 was determined at +25 mV, consistent with a single binding site for 94-IAA. A K_d = 5.90 μM at +25 mV was determined from the occupancy *vs.* concentration curve (Fig. 7*B;* left panel at bottom). At −25 mV, a Hill coefficient of 1.06 was calculated and a K_d = 5.13 μM. This anionic blocker thus appears to have a voltage-independent affinity for the channel. As shown in Fig. 7*B*, the inhibition by 94-IAA was reversed when the *cis* and *trans* baths were perfused with drug-free buffer.

Various divalent cations were examined for effects on the GCP Cl^- channel. Ca^{2+} and Mg^{2+} were without effect when applied to either channel surface at concentrations as high as 20 and 2 mM, respectively. Inhibition by extracellular Zn^{2+} was tested and the results are shown in Fig. 7*C*. Zn^{2+} reduced single channel conductance and induced an additional degree of flicker, as described by Franciolini and Nonner (1987) for the block of rat hippocampal neuron Cl^- channel by Zn^{2+}.

Discussion

The GCP Cl^- channels are spontaneously active upon reconstitution into planar lipid bilayers in the apparent absence of any soluble activators. No GABA was added to either solution, and the nominal Ca^{2+} concentration was zero for all experiments which were performed in the absence of added Ca^{2+}, and in the presence of 200 μM of either EGTA or citrate. Moreover, the addition of Ca^{2+} at up to 20 mM to the cytoplasmic surface of the channel had no effect. Thus, the GCP Cl^- channel can be excluded from the GABA-activated and Ca^{2+}-activated groups of Cl^- channels. This effectively places them in the category of leak channels discussed in the Introduction.

The GCP Cl^- channels display properties typical of other anion-selective leak channels: (i) spontaneous gating characterized by frequent brief closures (Bridges et al., 1987) and some modulation by voltage (Franciolini & Nonner, 1987; Reinhardt et al., 1987); (ii) an outwardly rectifying current-voltage relationship (Gögelein, 1988); (iii) a permeability-selectivity sequence that follows sequence I of Wright and Diamond (1977; Franciolini & Petris, 1990); and (iv) inhibition by the common stilbene inhibitors of Cl^- channels (Gögelein, 1988). The GCP Cl^- channel was also blocked by Zn^{2+}, as has been reported for neuronal Cl^- channels (Franciolini & Nonner, 1987) and amphibian skeletal muscle (Woll et al., 1987). Inhibition by the Cl^- channel ligand 94-IAA (Landry et al., 1989) was also demonstrated.

Two of these characteristics merit further comment. First, the direction of current rectification was assumed to be like that described for most small conductance Cl^- channels. We believe that this assumption is valid for the following reasons: in a review of the literature, Gögelein (1988) reported on the rectification properties of various Cl^- channels. Out of a total of 17 different Cl^- channels, 10 were outwardly rectifying, 6 did not rectify, and only 1 was inwardly rectifying (Gögelein, 1988; *cf.* Table 2). Moreover, during our studies of Na^+ channels (whose sidedness can be defined using guanidinium toxins) reconstituted from this same preparation

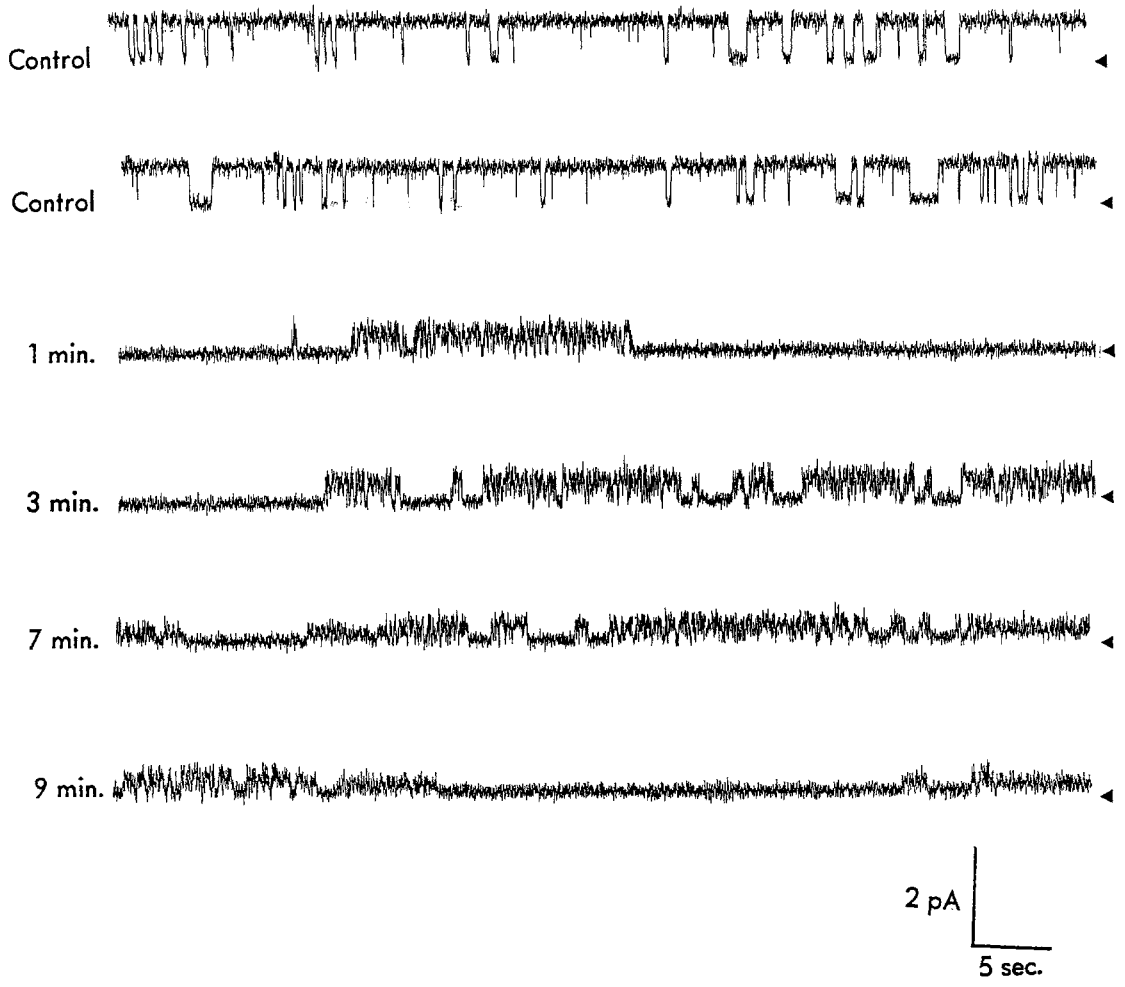

Fig. 6. DIDS block of GCP chloride channel. DIDS (100 μM) was applied to the external surface of a GCP Cl^- channel held at −30 mV. The two control records are consecutive current traces before the addition of 100 μM DIDS. In the remaining four records, the time of exposure to DIDS is given to the left of each trace. The zero current level is indicated by the single arrowhead in each instance. Ionic conditions were symmetric 200 mM NaCl, 10 mM HEPES, 0.2 mM EGTA.

(Wood et al., 1992), we noted that 13 of 18 channels (72%) incorporated into the bilayer backwards (i.e., with the extracellular surface facing *trans*). In agreement, for the Cl^- channels we studied, 25/38, or 66% incorporated with what we consider to be the extracellular surface facing the *trans* bath. Finally, we have previously reported that both the venom of the scorpion *Leiurus quinquestriatus* (DeBin & Strichartz, 1991) and a peptide toxin purified from that venom (DeBin, Maggio & Strichartz, 1993) inhibit rat colonic enterocyte Cl^- channels but only when applied to the cytoplasmic surface. This same venom was also found to inhibit the GCP Cl^- channel, but only from what is considered to be the cytoplasmic surface. For these reasons we believe that the GCP anion channel is outwardly rectifying.

Although the high value obtained for P_{Na}/P_{Cl} might at first seem unusual, several Cl^--selective channels have been reported to have considerable permeability to cations. Chloride channels from hippocampal neurons (P_{Na}/P_{Cl} = 0.25; Franciolini & Nonner 1987) and rat colon (P_{Na}/P_{Cl} = 0.11; Reinhardt et al., 1987) both have demonstrated the ability to conduct cations to a significant degree. Franciolini and Nonner (1987) have attempted to explain these results by the copermeation of cations and anions.

Given the prevalence of Cl^- channels, the possibility exists that the Cl^- channel reconstituted from the GCP preparation may in fact be derived from a non-neuronal source. However, by morphological and biochemical criteria, growth cone-derived elements are highly enriched and glial material (based on the markers, glial fibrillary acidic protein and the RC2 antigen) has been largely removed from the GCP preparation (Pfenninger et al., 1991; K. Lohse et al., *in preparation*). Therefore, Cl^- channels should be enriched in the GCP fraction if they are of growth cone origin. From the results of the incorporation rate studies (*summarized in*

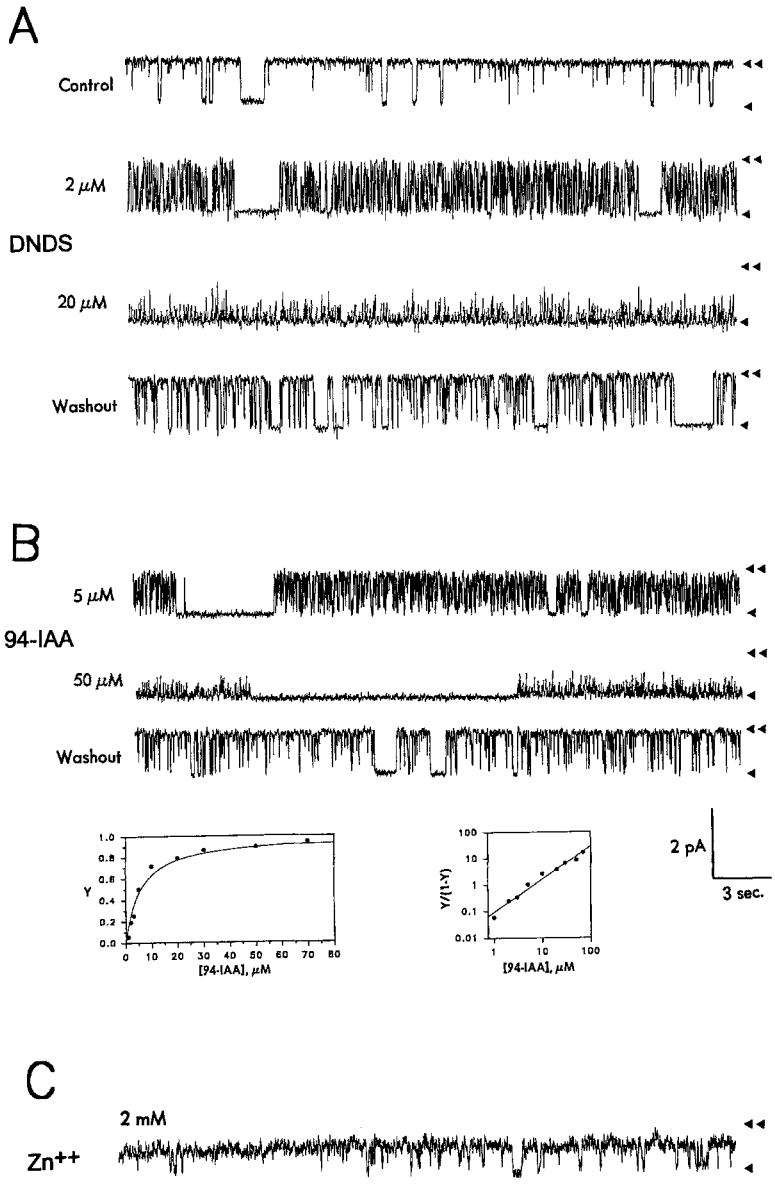

Fig. 7. GCP chloride channel inhibition by DNDS, 94-IAA, and Zn^{2+}. The control record shows a single GCP Cl^- channel in symmetric 200 mM NaCl, phosphate/citrate buffer, voltage clamped at +25 mV. Open channel and zero current levels are indicated by double and single arrowheads, respectively, to the right of each record (*Control* and Panels *A–C*). All records are filtered at 50 Hz low pass. Currents immediately after 2 or 20 μM DNDS applied to the extracellular channel surface, and after perfusion of the extracellular bath with six volumes of fresh buffer (washout). (*B*) Current traces from a channel *different* from that shown in Panel *A*, immediately thereafter 94-IAA was supplied to *both* sides of the bilayer to the concentrations indicated, and after perfusion of both the intracellular and extracellular baths with 8 volumes each of fresh buffer. The current traces at 5 and 50 μM were selected because they each have closings of substantial duration which allow the baseline, zero current level to be seen clearly. The presence of the ligand did *not* noticeably increase the frequency of these long closures. Ionic conditions were as in Panel *A*, and V_m = +25 mV. The Hill plot and occupancy-concentration curve were constructed as described in Materials and Methods using data from two separate experiments. (*C*) Current trace from a third GCP Cl^- channel at +30 mV after the addition of Zn^{2+} to the extracellular channel surface to a final concentration of 2 mM.

Table 1), it is clear that with each step of the purification process anion channel activity increases, a result consistent with the GCPs *per se* being the source of the channel. Although these experiments alone do not rigorously exclude the possibility that the GCP Cl^- channel derives from some other membrane source, considering the purity of the GCP preparation as it is described in Materials and Methods, this possibility seems unlikely. Furthermore, the most likely source of contaminating membranes in the developing brain would be glia. Cultured glial cells are known to have large conductance (>400 pS), ligand-insensitive Cl^- channels (Gray, Bevan & Ritchie, 1984; Sonnhof, 1987). One paper reports small conductance Cl^- channels from cultured glial cells of the rat optic nerve (Barres, Chun & Corey, 1988), but in these cells the small conductance channels coexist with large Cl^- channels. That no large conductance Cl^- channels were reconstituted from the GCP preparation argues against significant contamination from glial membranes of the type described by Barres et al. (1988).

The question concerning the source of the GCP Cl^- channel can be extended to the source of the channel within the GCP itself. The GCPs used for these reconstitution studies contain a variety of subcellular organelles. In particular, they contain mitochondria, agranular endoplasmic reticulum, and an abundance of various membrane vesicles, mostly plasmalemmal precursor vesicles. The possibility thus exists that the GCP Cl^- channel might originate from an intracellular

source. Anion channels from the endoplasmic reticulum and from the inner and outer mitochondrial membranes have been described (Schein, Colombini & Finkelstein, 1976; Sorgato, Keller & Stühmer, 1987; Schmid et al., 1988; Wunder & Colombini, 1991). In each case, however, regardless of the species from which the channels derive, the single channel characteristics differ widely from those described here.

Small conductance (≈20 pS) Cl^- channels have been reconstituted into planar lipid bilayers from the secretory vesicles purified from the rat and bovine neurohypophysis (Stanley, Ehrenstein & Russell, 1988; Lemos, Ocorr & Nordman, 1989). Barasch et al. (1988) reported an increase in Cl^- conductance in the vesicles of thyroid parafollicular cells in response to thyrotropin. Lemos et al. (1989) proposed that an increase in Cl^- current of the vesicular membrane increases Cl^- concentration within these vesicles. The elevated $[Cl^-]$ in turn is proposed to create an osmotic pressure drawing H_2O into the vesicle interior and thus causing it to swell. This swelling then triggers the release of the contents of vesicles adhering to the inside of the plasma membrane.

This hypothetical secretory role for Cl^- channels may have an analog in neurite outgrowth. Growth cones are involved in the dynamic process of plasmalemma expansion. Therefore, it can be expected that they would rapidly incorporate membrane from internal stores. Lockerbie, Miller and Pfenninger (1991) have confirmed this by inducing the exocytosis of vesicles from within the interior of intact GCPs. By measuring wheat germ agglutinin binding, they were able to detect an expansion of the GCP plasmalemma surface area, in response to K^+ depolarization, concomitant with a reduction of the number of internal, large, clear vesicles. The GCP Cl^- channel may serve to increase $[Cl^-]$ in these vesicles, and thus promote vesicle incorporation into the growing plasmalemma of the growth cone analogous to the vesicular fusion/release model of Lemos et al. (1989).

A different role for Cl^- channels in neurite outgrowth is suggested by the observation of Franciolini and Nonner (1987), who described an anion channel derived from 18-day-old embryonic rat hippocampal neurons. The single channel conductance, halide selectivity sequence, gating characteristics and sensitivity to Zn^{2+} observed for this channel were nearly identical to those of the GCP Cl^- channel described here. These authors proposed that this channel might be involved in reducing excitability in these cells by stabilizing membrane potential at or near E_{Cl}. The GCP Cl^- channel may have the same function in growth cones. Cohan and Kater (1986) have reported that repetitive stimulation of neurons from *Helisoma* suppresses neurite outgrowth. Thus in suppressing excitability, the GCP anion channel located in the plasmalemma may promote neurite outgrowth.

This research was financially supported by Public Health Service grants GM15904 (to G.R.S.) and NS24676 (to K.H.P.).

The authors thank Dr. Donald Landry, Columbia University, for the generous gift of 94-IAA, and Prof. Dale Benos, University of Alabama, for helpful suggestions on chloride channel pharmacology made during the experiments. Drs. Stephen Raymond and G.K. Wang of the Anesthesia Research Laboratories of The Brigham and Women's Hospital are acknowledged for providing us with an amplifier and laser printer necessary for the construction of many of the figures. Ms. Ellen Jacobson helped with the manuscript typing.

References

Bader, C.R., Bertrand, D., Schlichter, R. 1987. Ca^{++}-activated chloride current in cultured sensory and parasympathetic quail neurones. *J. Physiol.* **394:**125–148

Barasch, J., Gershon, M.D., Nunez, E.A., Tamir, H., Al-Awqati, Q. 1988. Thyrotropin induces the acidification of the secretory granules of parafollicular cells by increasing chloride conductance. *J. Cell Biol.* **107:**2137–2147

Barres, B.A., Chun, L.L.Y., Corey, D.P. 1988. Ion channel expression by white matter glia. *Glia* **1:**10–30

Bear, C.E. 1988. Phosphorylation-activated chloride channels in human skin fibroblasts. *FEBS Lett.* **237:**145–149

Blatz, A.L., Magleby, K.L. 1983. Single voltage-dependent chloride-selective channels of large conductance in cultured rat muscle. *Biophys. J.* **43:**237–241

Blatz, A.L., Magleby, K.L. 1985. Single chloride-selective channels active at resting membrane potentials in cultured rat skeletal muscle. *Biophys. J.* **47:**119–123

Bridges, R.J., Worrell, R.T., Frizzell, R.A., Benos, D.J. 1987. Stilbene disulfonate blockade of colonic secretory Cl^- channels in planar lipid bilayers. *Am. J. Physiology* **256:**C902–912

Cliff, W.H., Frizzell, R.A. 1990. Separate Cl^- conductances activated by cAMP and Ca^{2+} in Cl^--secreting epithelial cells. *Proc. Natl. Acad. Sci USA* **87:**4956–4960

Cohan, C.S., Kater, S.B. 1986. Suppression of neurite elongation and growth cone motility by electrical activity. *Science* **232:**1638–1640.

Cohen, R.S., Blomberg, F., Berzins, K., Siekevitz, P. 1977. The structure of postsynaptic densities isolated from dog cerebral cortex. *J. Cell Biol.* **74:**181–203

DeBin, J.A., Maggio, J.E., Strichartz, G.R. 1993. Purification and characterization of chlorotoxin, a chloride channel ligand from the venom of the scorpion *Leiurus quinquestriatus. Am. J. Physiol.* **264:**C361–369

DeBin, J.A., Strichartz, G.R. 1990. Anion channels from mammalian nerve growth cones. *Biophys. J.* **57:**319*a* (*Abstr.*)

DeBin, J.A., Strichartz, G.R. 1991. Chloride channel inhibition by the venom of the scorpion *Leiurus quinquestriatus. Toxicon* **29:**1403–1408

Diener, M., Rummel, W., Mestres, P., Lindemann, B. 1989. Single chloride channels in colon mucosa and isolated colonic enterocytes of the rat. *J. Membrane Biol.* **108:**21–30

Dudel, J., Franke, C., Hatt, H., Usherwood, P.N.R. 1989. Chloride channels gated by extrajunctional glutamate receptors (H-receptors) on locust leg muscle. *Brain Res.* **481:**215–220

Franciolini, F., Nonner, W. 1987. Anion and cation permeability of a chloride channel in rat hippocampal neurons. *J. Gen. Physiol.* **90:**453–478

Franciolini, F., Petris, A. 1990. Chloride channels of biological membranes. *Biochim. Biophys. Acta* **103:**247–259

Franke, C., Hatt, H., Dudel, J. 1986. The inhibitory chloride channel activated by glutamate as well as gamma-amino-butyric acid (GABA). *J. Comp. Physiol. A.* **159:**591–660

Frizzell, R.A. 1988. The role of absorptive and secretory processes in the airway surface. *Am. Rev. Respir. Dis.* **139:**S3–S6

Gray, P.T.A., Bevan, S., Ritchie, J.M. 1984. High conductance anion-selective channels in rat cultured Schwann cells. *Proc. Roy. Soc. Lond.* **B221:**395–409

Gögelein, H. 1988. Chloride channels in epithelia. *Biochim. Biophys. Acta* **947:**109–156

Hanrahan, J.W., Tabcharani, J.A. 1990. Inhibition of an outwardly rectifying anion channel by HEPES and related buffers. *J. Membrane Biol.* **116:**65–77.

Hayslett, J.P., Gögelein, H., Kunzelmann, K., Greger, R. 1987. Characteristics of apical chloride channels in human colon cells (HT_{29}), *Pfluegers Arch.* **410:**487–494

Hille, B. 1992. Ion Channels of Excitable Membranes. 2nd Ed. Sinauer, Sunderland, MA

Kolb, H.A., Brown, C.D.A., Murer, H. 1985. Identification of a voltage-dependent anion channel in the apical membrane of a Cl^--secretory epithelium (MDCK). *Pfluegers Arch.* **403:**262–265

Krnjevic, K. 1974. Chemical nature of synaptic transmission in vertebrates. *Annu. Rev. Physiol.* **54:**418–505

Landry, D.W., Akabas, M.H., Redhead, C., Edelman, A., Cragoe, E.J., Jr., Al-Awqati, Q. 1989. Purification and reconstitution of chloride channels from kidney and trachea. *Science* **244:**1469–1472

Lemos, J.R., Ocorr, K.A., Nordman, J.J. 1989. Possible role for ionic channels in neurosecretory granules of the rat neurohypophysis. *In:* Secretion and its Control. G.S. Oxford, editor. pp. 333–348. Rockefeller University, NY

Lewis, C.A. 1979. Ion-concentration dependence of the reversal potential and the single channel conductance of ion channels at the frog neuromuscular junction, *J. Physiol.* **286:**417–445

Lockerbie, R.O., Miller, V.E., Pfenninger, K.H. 1991. Regulated plasmalemmal expansion in nerve growth cones. *J. Cell. Biol.* **112:** 1215–1227

Lowry, O.H., Rosebrough, N.J., Farr, A.L., Randall, R.J. 1951. Protein measurement with the folin phenol reagent. *J. Biol. Chem.* **193:**265–275

Lukacs, G.L., Moczydlowski, E. 1990. A chloride channel from lobster walking leg nerves: Characterization of single-channel properties in planar bilayers. *J. Gen. Physiol.* **96:**707–733

Nomura, K., Sokabe, M. 1991. Anion channels from rat brain synaptosomal membranes incorporated into planar bilayers. *J. Membrane Biol.* **124:**53–62

Owen, D.G., Segal, M., Barker, J.L. 1984. A Ca^{++}-dependent Cl^- conductance in cultured mouse spinal neurons. *Nature* **311:**567–570

Pfenninger, K.H., de la Houssaye, B.A., Frame, L., Helmke, S., Lockerbie, R.O., Lohse, K., Miller, V., Negre-Aminou, P., Wood, M.R. 1991. Biochemical dissection of plasmalemmal expansion at the growth cone. *In:* The Nerve Growth Cone. P.C. Letourneau, S.B. Kater, and E.R. Macagno, editors. pp. 111–123. Raven, NY

Pfenninger, K.H., Ellis, L., Johnson, M.P., Friedman, L.B., Somlo, S. 1983. Nerve growth cones isolated from fetal rat brain: subcellular fractionation and characterization. *Cell* **35:**573–584

Reinhardt, A., Bridges, R.J., Rummel, W., Lindermann, B. 1987. Properties of an anion-selective channel from rat colonic enterocyte plasma membranes reconstituted into planar phospholipid bilayers. *J. Membrane Biol.* **95:**47–54

Robinson, R.A., Stokes, R.H. 1959. Electrolyte Solutions. 2nd ed. Butterworth's, London

Sattelle, D.B. 1992. Receptors for L-glutamate and GABA in the nervous system of an insect. *Comp. Biochem. Physiol. C.* **103:**429–438

Schein, S.J., Colombini, M.J., Finkelstein, A. 1976. Reconstitution in planar lipid bilayers of a voltage-dependent anion-selective channel obtained from *Paramecium* mitochondria. *J. Membrane Biol.* **30:**99–120

Schmid, A., Gögelein, H., Kemmer, T.P., Schulz, I. 1988. Anion channels in giant liposomes made of endoplasmic reticulum vesicles from rat exocrine pancreas. *J. Membrane Biol.* **104:**275–282

Segal, M., Barker, J.L., Owen, D.G. 1987. Chloride conductances in central neurons. *Israel J. Med. Sci.* **23:**95–100

Sonnhof, U. 1987. Single voltage-dependent K^+ and Cl^- channels in cultured rat astrocytes. *Can. J. Physiology* **65:**1043–1050

Sorgato, M.C., Keller, B.U., Stühmer, W. 1987. Patch-clamping of the inner mitochondrial membrane reveals a voltage-dependent ion channel. *Nature* **330:**498–500

Stanley, E.F., Ehrenstein, G., Russell, J.T. 1988. Evidence for anion channels in secretory vesicles. *Neuroscience* **25:**1035–1039

Takeuchi, A., Takeuchi, N. 1964. Iontophoretic application of gamma aminobutyric acid on crayfish muscle. *Nature* **203:**494–497

Takeuchi, A., Takeuchi, N. 1966. On the permeability of the presynaptic terminal of the crayfish neuromuscular junction during synaptic inhibition, *J. Physiol.* **183:**433–449

Welsh, M.J., Anderson, M.P., Rich, D.P., Berger, H.A., Denning, G.M., Ostedgaard, L.S., Sheppard, D.N., Cheng, S.H., Gregory, R.J., Smith, A.E. 1992. Cystic fibrosis transmembrane conductance regulation: a chloride channel with novel regulation. *Neuron* **8:**821–829.

Woll, K.H., Leibowitz, M.D., Neumcke, B., Hille, B. 1987. A high conductance anion channel in adult amphibian skeletal muscle. *Pfluegers Arch.* **410:**632–640

Wood, M.R., DeBin, J.A., Strichartz, G.R., Pfenninger, K.H. 1992. Plasmalemmal insertion and modification of sodium channels at the nerve growth cone. *J. Neurosci.* **12:**2948–2959

Wright, E.M., Diamond, J.M. 1977. Anion selectivity in biological systems. *Physiol. Rev.* **57:**109–156

Wunder, U.R., Colombini, M. 1991. Patch clamping VDAC in liposomes containing whole mitochondrial membranes. *J. Membrane Biol.* **123:**83–91

Yamamoto, D., Suzuki, N. 1987. Blockage of chloride channels by HEPES buffer. *Proc. Roy. Soc. Lond.* **B230:**93–100

APPENDIX

Equations Used for the Determination of Permeability Ratios

Equation (A1) is the Goldman, Hodgkin Katz equation taken from Hille (1992):

$$V_o = \frac{RT}{F} \ln \frac{P_{Na}[Na^+]_o + P_{Cl}[Cl^-]_i + P_A[A^-]_i}{P_{Na}[Na^+]_i + P_{Cl}[Cl^-]_o + P_A[A^-]_o} \tag{A1}$$

Equation (A2) was adapted from Lewis (1979):

$$V_o = \frac{RT}{F} \ln \frac{P_{Na}[Na^+]_o + P_{Cl}[Cl^-]_i + 4P_{A'}[A^=]_i}{P_{Na}[Na^+]_i + P_{Cl}[Cl^-]_o + 4P_{A'}[A^=]_o \exp(-FV_o/RT),} \tag{A2}$$

where $P_A = P_{A'}(1 + \exp(-FV_o/RT))$
V_o = reversal potential (E_{rev})
P_{Na}, P_{Cl}, P_{A^-} = permeability coefficients for Na^+, Cl^-, and test anion
$[Na^+]_i$ = concentration of Na^+ in internal solution
$[Na^+]_o$ = concentration of Na^+ in external solution
$[Cl^-]_i$ = concentration of Cl^- in internal solution
$[Cl^-]_o$ = concentration of Cl^- in external solution
$[A^-]_i$ = concentration of monovalent test anion in internal solution
$[A^-]_o$ = concentration of monovalent test anion in external solution
$[A^=]_i$ = concentration of divalent anion in internal solution
$[A^=]_o$ = concentration of divalent anion in external solution
F = Faraday constant
R = Gas constant
T = Absolute temperature
Note that activity coefficient terms are not shown in Eqs. (A1) and (A2) but, except where noted, are assumed equal to unity.